SUPPLEMENTARY INFORMATION

Radiation-grafted anion-exchange membranes: key features for enhanced water electrolysis

Ana Laura G. Biancolli[§a,b], Binyu Chen[§b], Alessandra S. Menandro[b], Fabio C. Fonseca[a], Elisabete I. Santiago[a]*, and Steven Holdcroft[b]*

a. Nuclear and Energy Research Institute, IPEN/CNEN, 05508-000, São Paulo, Brazil

b. Department of Chemistry, Simon Fraser University, Burnaby, V5A 1S6, Canada

[§]These authors equally contributed to this work.
*Corresponding Authors: elisabete.santiago@usp.br ; holdcrof@sfu.ca

Radiation-grafted anion-exchange membrane (RIG-AEM) synthesis

Radiation-grafted anion-exchange membranes (RIG-AEMs) were prepared using low-density polyethylene (LDPE) or ethylene-tetrafluoroethylene (ETFE) as starting films as follows: LDPE biaxially oriented films (Goodfellow, 25 µm, 50 µm or 125 µm thick) or ETFE films (Nowfol, 25 µm or 50 µm thick) were irradiated in an e-beam (EB) accelerator in air at ~ -10 °C by placing the pristine films over a layer of dry ice. A Dynamitron Continuous Electron Beam Unit from RDI – Radiation Dynamics Inc. USA, model DC 1500/25/4 - JOB 188 with 1.5 MeV of maximum energy was used. The polymer films were exposed to different radiation absorbed doses: 20-100 kGy. Irradiation was performed at 10 kGy per step and higher doses obtained by sequential steps, with a dose rate of 39.97 kGy s^{-1}. The radiation penetration was calculated using the film's density and thickness and the energy used was 0.55 MeV with an EB current of 5.74 mA. The irradiated samples were stored under air in a temperature-controlled freezer at -40 °C for a maximum period of 7 days.

For the grafting step, pre-irradiated LDPE or ETFE films were weighted and immersed in an aqueous solution containing 5% (v/v) of 3,4-vinylbenzyl chloride (3,4-VBC, 90%, Sigma-Aldrich), and 1% (v/v) of surfactant 1-octyl-2-pyrrolidone (Sigma-Aldrich). The mixture was deoxygenated by

purging with N_2 for 1 h, sealed and heated to 55 °C for 5 h for LDPE films and 70 °C for 16 h for ETFE films. The resultant VBC-grafted films were removed from solution and washed thoroughly with toluene and acetone, followed by drying at room temperature (LDPE films) or 50 °C (ETFE films) for 5 h in a vacuum oven.

Amination was carried out by immersing the VBC-grafted LDPE or ETFE films in aqueous trimethylamine (TMA) solution (~ 45% vol., Sigma-Aldrich). Samples were kept in TMA solution under stirring for 24 h followed by washing in fresh ultra-pure water at 50 °C for 1 h. Membranes were converted to their Cl^- form by immersion in aqueous NaCl (1 M) overnight with two additional exchanges of solutions, before storing in fresh ultra-pure water.

Main characteristics of synthesized AEMs

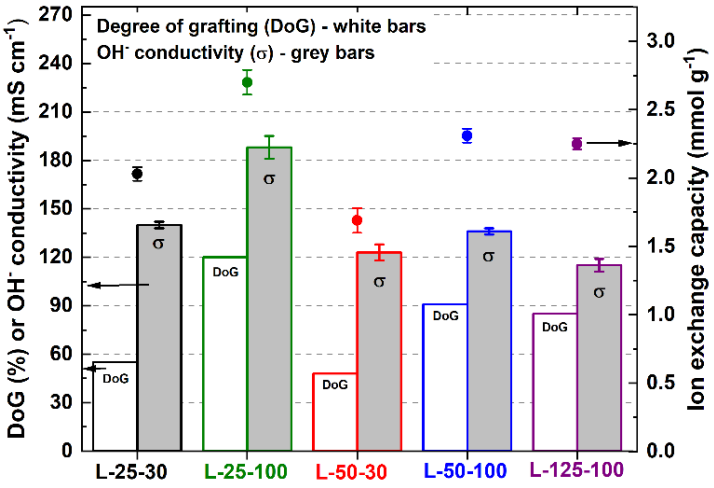

Figure S1. Graphical representation of Table 1 data for better visualization. Degree of grafting (DoG), ion-exchange capacity (IEC), and OH^- conductivity of LDPE-based RIG-AEMs.

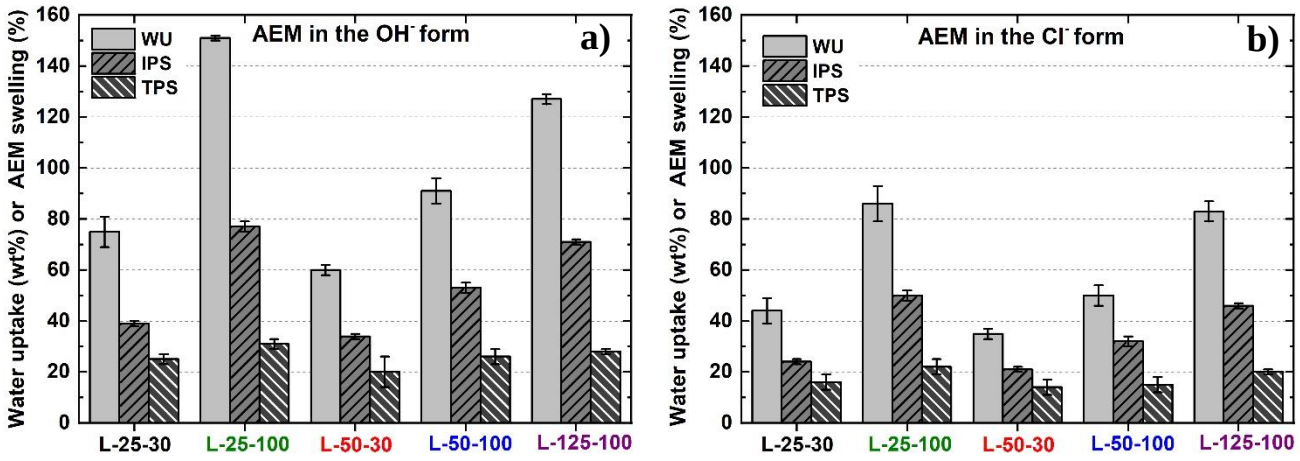

Figure S2. Water uptake (WU), in-plane swelling (IPS), and through-plane swelling (TPS) of **(a)** LDPE-based RIG-AEMs in the OH^- form, **(b)** LDPE-based RIG-AEMs in the Cl^- form, after 24 h immersed in ultra-pure water at RT.

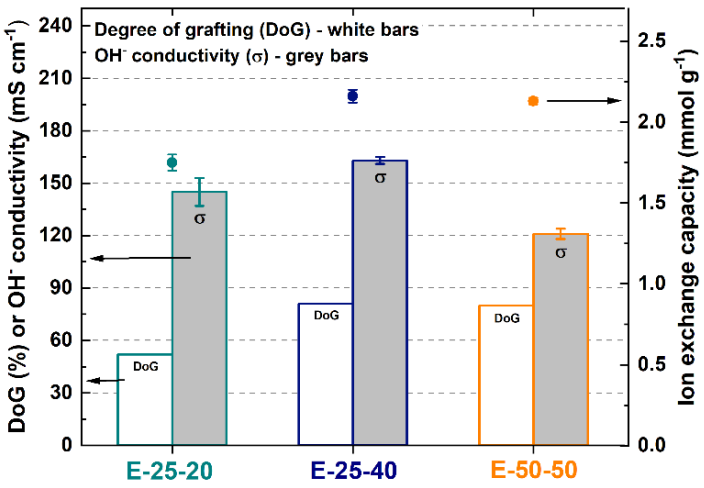

Figure S3. Graphical representation of Table 2 data for better visualization. Degree of grafting (DoG), ion-exchange capacity (IEC), and OH^- conductivity of ETFE-based RIG-AEMs.

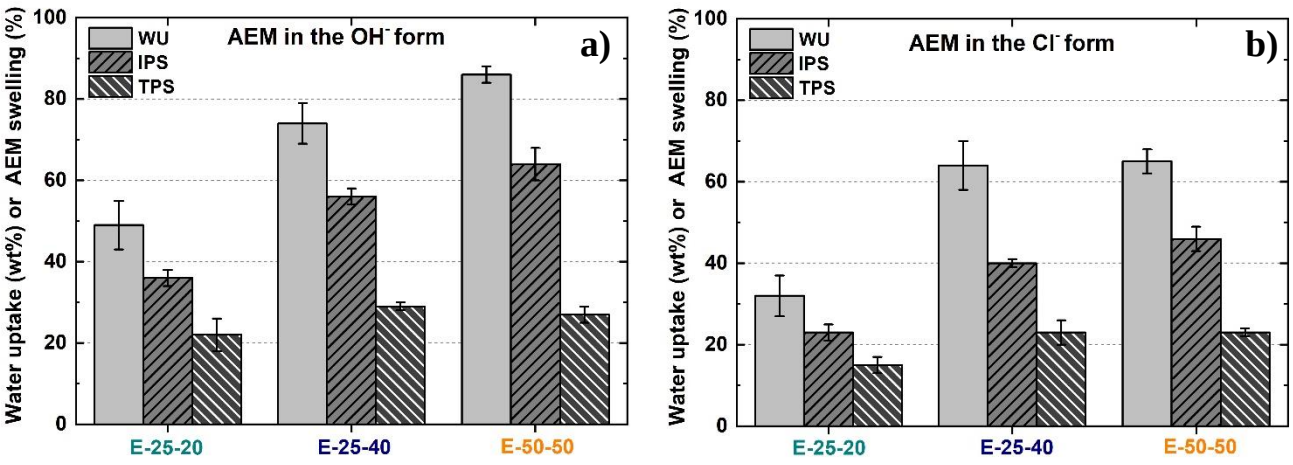

Figure S4. Water uptake (WU), in-plane swelling (IPS), and through-plane swelling (TPS) of **(a)** ETFE-based RIG-AEMs in the OH^- form, **(b)** ETFE-based RIG-AEMs in the Cl^- form, after 24 h immersed in ultra-pure water at RT.

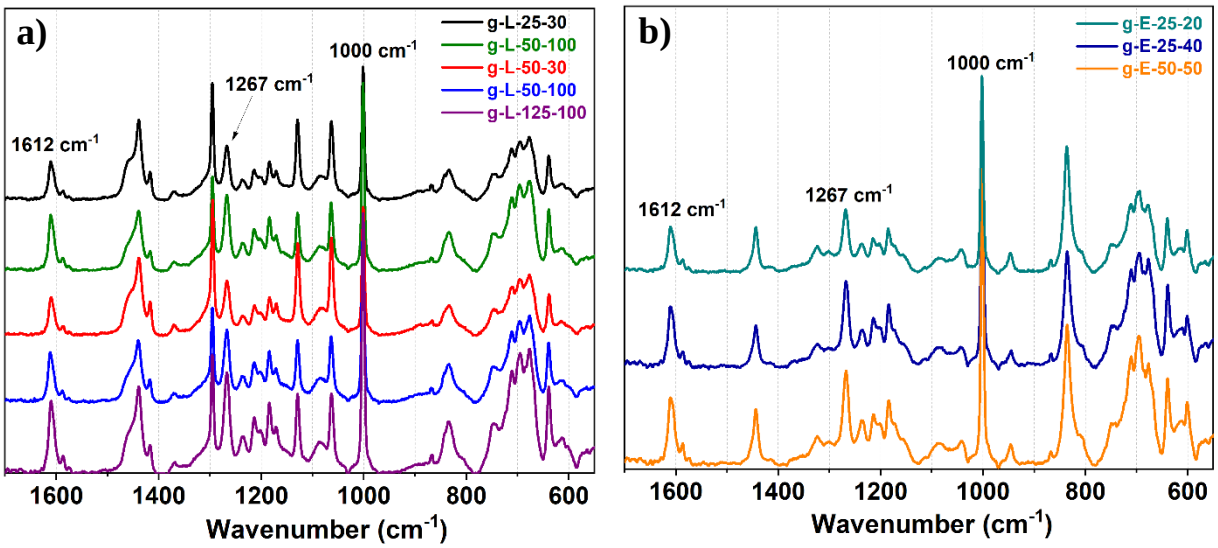

Figure S5. Raman spectra of a) VBC-grafted LDPE films irradiated with 30 or 100 kGy, derived from the 25, 50, or 125 µm thick pristine films; b) VBC-grafted ETFE films irradiated with 20, 40 or 50 kGy, derived from the 25 or 50 µm thick pristine films. Laser λ = 785 nm

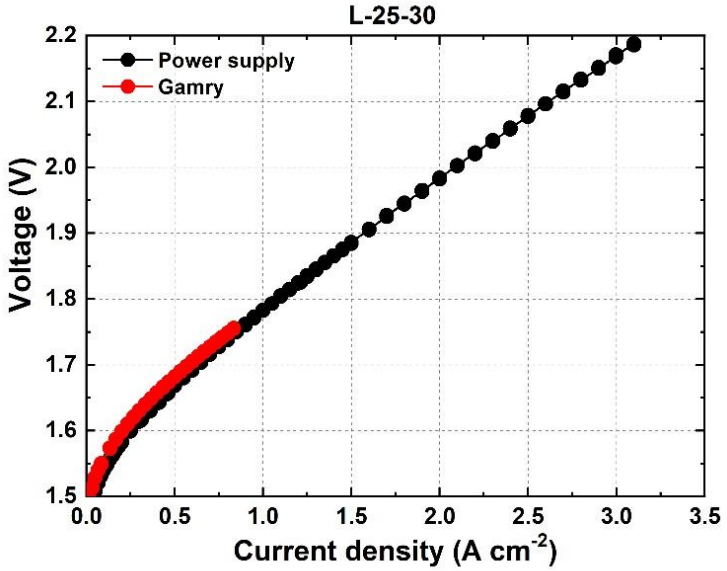

Figure S6. Example of polarization curves of two water electrolyzers containing L-25-30 AEM with two distinct batches of electrodes, acquired in two different equipment, and by two different operators. The red data points were obtained in a Gamry Interface 5000E, which can reach a maximum current of 5 A, while the black data points were obtained using a DC power supply Keithley 2260B-30-36 with maximum achievable current of 36 A. Anode: stainless steel felt only. Cathode: Pt/C (80 wt % catalyst and 20 wt % AP1-HNN8-00-X ionomer, Ionomr Innovations Inc) coated on Ni Felt (CCS). Experiments were conducted in 1 M KOH at 60 °C with a flow rate of 5 mL min^{-1}.

Tensile tests

The mechanical properties of the two most promising RIG-AEMs of this work (L-50-30 and E-25-20) were analyzed by uniaxial tensile testing using an Instron 3344 series single column system at ambient conditions, room temperature and RH, with a stretching speed of 2 mm min^{-1}. Rectangular samples (1 × 5 cm^2) were dried in a vacuum oven at 50 °C prior to measurements. The elongation at break and Young's modulus reported in Figure S7 represent the average of at least five sample measurements, with the error represented as the standard deviation.

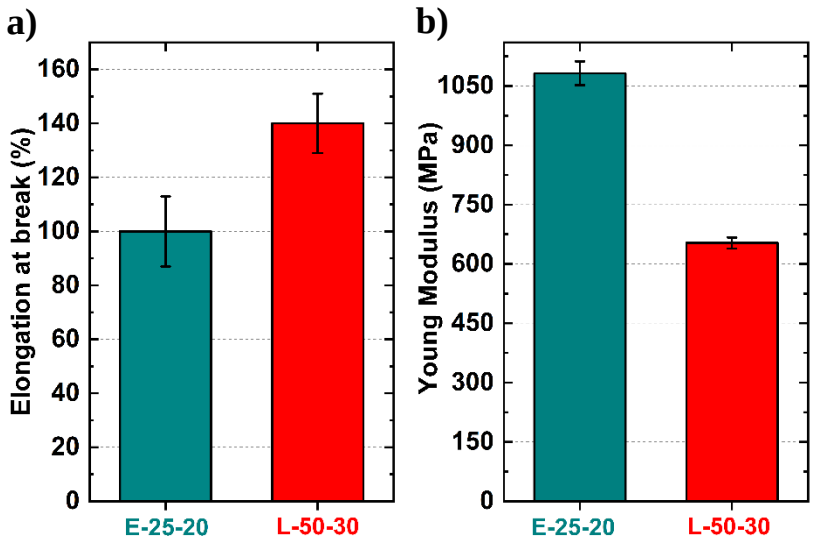

Figure S7. Mechanical properties of the E-25-30 and L-50-30 RIG-AEMs: a) Elongation at break; b) Young's modulus.

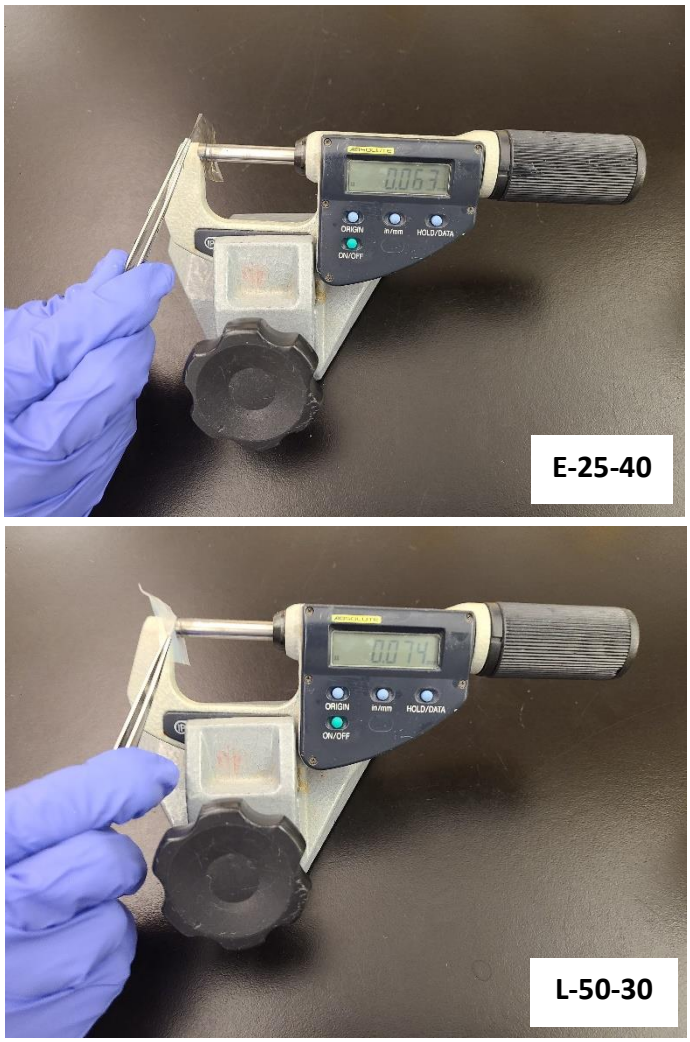

Figure S8. Two examples on how the thickness of each membrane was measured.

Table S1. Detailed membrane/electrode assembly from Figure 8. CCS = catalyst coated substrate, CCM = catalyst coated membrane.

Number in Fig. 8	AEM	AEM dry thickness (µm)	Anode catalyst/PTL	Cathode catalyst/PTL	Ionomer/binder	MEA type	KOH flow rate	Reference
1	HTMA-DAPP	26	NiFe nanofoam	PtRu/C SGL 29 BC	-	CCS	-	[1]
2	Sustanion 37-50	50	IrO_2	Pt/C	-	-	-	[2]
3	AF1-HNN8-50	50	Ir black / Titanium PTL	Pt/C Carbon paper	FAA-3-SOLUT-10	CCS	-	[3]
4	AF2-HWP8-75-X	85	SS felt	Pt/C / Ni felt	AP2-HNN8-00-X	CCM	5 mL min^{-1}	[4]
5	AF1-HNN8-50	50	SS felt	Pt/C / Ni felt	AF1-HNN8-50	CCM	5 mL min^{-1}	[4]
6	FAA-3-PK-75	75	SS felt	Pt/C / Ni felt	FAA-3-SOLUT-10	CCM	5 mL min^{-1}	[4]
7	AF3-HWK9-75-X	75	SS felt	Pt/C / Ni felt	AP3-HNN9-00	CCM	5 mL min^{-1}	[4]
8	AF1-HNN8-50	50	SS felt	Pt/C / Ni felt	AF1-HNN8-50	CCS	5 mL min^{-1}	[4]
9	Celazole PBI	50	$NiFe_2O_4$ / SS felt	NiFeCo / Carbon paper	Nafion	CCS	2 mL min^{-1}	[5]
10	AMI-7001	450	$NiFe_2O_4$ / SS felt	NiFeCo / Carbon paper	Nafion	CCS	2 mL min^{-1}	[5]
11	Fumatech FAS-50	50	$NiFe_2O_4$ / SS felt	NiFeCo / Carbon paper	Nafion	CCS	2 mL min^{-1}	[5]
12	HTMA-DAPP	50	IrO_2 / Platinized Titanium	PtRu/C / Carbon paper	HTMA-DAPP	-	100 mL min^{-1}	[6]
13	Fumatech FAA-3-50	50	IrO_2/ Ti GDL	Pt/C / Carbon paper	FAA-3-Br	CCM	1 mL min^{-1}	[7]
14	PVBC-MPy/35%PEK-cardo	60	NiFe-LDH / Ni Felt	MoNi/ Ni felt	PTFE	CCS	70 mL min^{-1}	[8]
15	HMT-PMBI	50	NiAlMo	NiAlMo	-	CCS	-	[9]
16	Sustanion	50	$NiFe_2O_4$ / Ni fiber	NiFeCo / SS fiber	5% Nafion	CCS	3-5 mL min^{-1}	[10]
17	Tukuyama A201	28	$NiFe_2O_4$ / Ni fiber	NiFeCo / SS fiber	5% Nafion	CCS	3-5 mL min^{-1}	[10]
18	AEMION	38	$NiFe_2O_4$ / Ni fiber	NiFeCo / SS fiber	5% Nafion	CCS	3-5 mL min^{-1}	[10]

REFERENCES

1 D. Li, E. J. Park, W. Zhu, Q. Shi, Y. Zhou, H. Tian, Y. Lin, A. Serov, B. Zulevi, E. D. Baca, C. Fujimoto, H. T. Chung and Y. S. Kim, *Nat. Energy*, 2020, **5**, 378–385.

2 J. J. Kaczur, H. Yang, Z. Liu, S. D. Sajjad and R. I. Masel, *Front. Chem.*, 2018, **6**, 1–16.

3 P. Fortin, T. Khoza, X. Cao, S. Y. Martinsen, A. Oyarce Barnett and S. Holdcroft, *J. Power Sources*, 2020, **451**, 227814.

4 B. Chen, A. L. G. Biancolli, C. L. Radford and S. Holdcroft, *ACS Energy Lett.*, 2023, 2661–2667.

5 Z. Liu, S. D. Sajjad, Y. Gao, H. Yang, J. J. Kaczur and R. I. Masel, *Int. J. Hydrogen Energy*, 2017, **42**, 29661–29665.

6 J. Liu, Z. Kang, D. Li, M. Pak, S. M. Alia, C. Fujimoto, G. Bender, Y. S. Kim and A. Z. Weber, *J. Electrochem. Soc.*, 2021, **168**, 054522.

7 J. E. Park, S. Y. Kang, S. H. Oh, J. K. Kim, M. S. Lim, C. Y. Ahn, Y. H. Cho and Y. E. Sung, *Electrochim. Acta*, 2019, **295**, 99–106.

8 H. Li, M. R. Kraglund, A. K. Reumert, X. Ren, D. Aili and J. Yang, *J. Mater. Chem. A*, 2019, **7**, 17914–17922.

9 L. Wang, T. Weissbach, R. Reissner, A. Ansar, A. S. Gago, S. Holdcroft and K. A. Friedrich, *ACS Appl. Energy Mater.*, 2019, **2**, 7903–7912.

10 I. V. Pushkareva, A. S. Pushkarev, S. A. Grigoriev, P. Modisha and D. G. Bessarabov, *Int. J. Hydrogen Energy*, 2020, **45**, 26070–26079.